LUND UNIVERSITY

Hybrid Control Techniques for Switched-Mode DC-DC Converters, Part II: The Step-Up Topology

Beccuti, A; Papafotiou, G; Morari, Manfred; Almer, S; Fujioka, H; Jönsson, Ulf; Kao, Chung-Yao; Wernrud, Andreas; Rantzer, Anders; Baja, M; Cormerais, H; Buisson, J

2007

[Link to publication]

Proceedings of the 2007 American Control Conference
Marriott Marquis Hotel at Times Square
New York City, USA, July 11-13, 2007

FrB16.6

Hybrid Control Techniques for Switched-Mode DC-DC Converters
Part II: The Step-Up Topology

A.G. Beccuti[†],
G. Papafotiou, M. Morari
ETH

S. Almér, H. Fujioka[!]
U. Jönsson, C.-Y. Kao[!]
KTH

A. Wernrud, A. Rantzer
LTH

M. Bâja, H. Cormerais and
J. Buisson
Supélec

Abstract— **Several recent techniques from hybrid and optimal control are evaluated on a power electronics benchmark problem. The benchmark involves a number of practically interesting operating scenarios for a fixed-frequency step-up dc-dc converter. The specifications are defined such that good performance can only be obtained if the switched and nonlinear nature of the problem is respected during the design phase.**

I. INTRODUCTION

In this paper we investigate the application of hybrid systems control design techniques to a class of power electronic systems, namely fixed frequency dc-dc converters. The system under consideration is a fixed-frequency step-up (boost) converter, operating in the continuous current mode. Part 1 of the paper covers the analysis and control synthesis of the related step-down (buck) converter.

Despite its simplicity, the step-up topology represents a good entry point for the investigation of the control design and performance benefits that can be brought by hybrid control techniques. As will be later highlighted, the control problem entails a number of challenges, such as the non-minimum phase behavior of the controlled variable and the existence of multiple steady-state equilibria, while the hybrid nature of the system and the existence of input constraints further complicate the control design task. The benchmark example investigated in this paper was first defined in [1] to which we also refer for a comprehensive survey of the state of the art works in the power electronics area.

Four research groups identified according to the affiliations (ETH, KTH, LTH, Supélec) have applied recent ideas from the hybrid control area to the benchmark. More specifically, ETH uses Model Predictive Control (MPC) based on a Piecewise Affine (PWA) discrete-time model, KTH proposes a controller designed with the $\mathcal{H}_\infty$ technique using a sampled-data model of the converter, LTH uses Relaxed Dynamic Programming based on representation of the converter as a Robust Piecewise Affine (RPWA) system and Supélec investigates the application of stabilizing Lyapounov-based control using a Port-Control Hamiltonian formulation of the continuous-time plant dynamics.

II. PHYSICAL MODEL OF THE STEP-UP CONVERTER

The topology of the step-up converter is shown in Fig. 1. Using normalized quantities, r_o denotes the output load
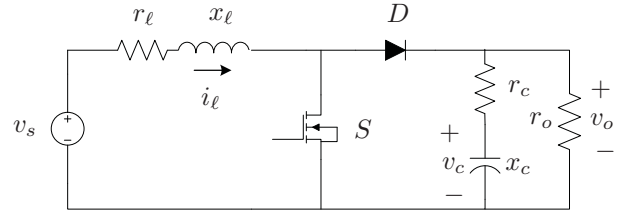
[†] Corresponding author. Email: beccuti@control.ee.ethz.ch
[!] Fujioka is with Kyoto University and Kao is with the University of Melbourne.

Fig. 1: Topology of the step-up (boost) converter

which we assume to be ohmic, r_c the Equivalent Series Resistance (ESR) of the capacitor, r_ℓ is the internal resistance of the inductor, x_ℓ and x_c represent the inductance and the capacitance of the low-pass filtering stage and v_s denotes the source voltage.

The switching stage of the converter comprises a controlled semiconductor switch S and a secondary switch D that is operated dually to the primary one. The switches are driven by a pulse sequence of constant frequency (period), the *switching frequency* f_s (*switching period* T_s), which characterizes the operation of the converter. The dc component of the output voltage can be regulated through the duty cycle (ratio) d, which is defined by $d = \frac{t_{on}}{T_s}$, where t_{on} represents the interval within the switching period during which the controlled switch is in conduction.

The state vector is given by $x(t) = [i_\ell(t) \; v_c(t)]^T$, comprising the inductor current and the capacitor voltage; the system is described by the following pair of affine continuous time state-space equations

$$\dot{x}(t) = \begin{cases} F_1 x(t) + f_1 v_s, & kT_s \leqslant t < (k+d[k])T_s \\ F_2 x(t) + f_2 v_s, & (k+d[k])T_s \leqslant t < (k+1)T_s \end{cases}$$
(1a)

$$v_o(t) = \begin{cases} g_1^T x(t), & kT_s \leqslant t < (k+d[k])T_s \\ g_2^T x(t), & (k+d[k])T_s \leqslant t < (k+1)T_s \end{cases}$$
(1b)

Matrices F_1 and F_2 and vectors f_1, f_2, g_1 and g_2 are of appropriate sizes and depend on the circuit parameters. Their analytical expressions can be found in [1].

Notice that the evolution of the system is externally affected by *when* the switching takes place; the input to the system is therefore the duty cycle $d[k]$ specifying the switching instant.

III. MODELLING FOR CONTROL DESIGN

The two milestone papers on the analysis and design of switch-mode dc-dc converters were written by Middlebrook and Cuk [2], [3]. In these, the basic ideas of state-space averaging were introduced and the so-called small signal modeling was proposed for control design purposes. The notion of averaging implies that only the dynamics of the dc components of the circuit variables are taken into account, which are by definition quite slow compared to the switching frequency. On the other hand, the term small signal analysis describes the linearization of the resulting non-linear state equations around the operating point. The averaging technique is convenient to use but it offers only a low frequency approximation of the true dynamics where the effect of discontinuous switching is ignored. Several alternative modeling techniques will be discussed in the paper, including both continuous and discrete time hybrid systems frameworks. Examples of the latter are Piecewise Affine (PWA) and Robust Piecewise Affine (RPWA) systems, Sampled Data (SD), and Port-Control Hamiltonian models.

A. ETH: Piecewise Affine (PWA) Systems

From an implementation point of view, it is preferable that all states used in the prediction model be directly measurable. Thus, the capacitor voltage is replaced by the output voltage in the state vector which leads to setting $x(t) = [i_\ell(t) \ v_o(t)]^T$. Additionally, to account for variations in the voltage source v_s directly, the (to be derived) optimal control law would need to be parameterized over v_s. To obviate this requirement and as will further be explained in section V-A, the voltage source v_s is removed from the model equations by redefining the scaled state vector $x'(t) = [i'_\ell(t) \ v'_o(t)] = [\frac{i_\ell(t)}{v_s} \ \frac{v_o(t)}{v_s}]$. Next, we formulate a discrete time model by employing a sampling interval equal to the switching period T_s. The employed method considers a direct least squares fitting (LSF) approximation over several regions of the control input of the exact system update equations, yielding a PWA description of the associated non-linear expressions. These can be written as

$$x'[k+1] = \Phi(d[k])x'[k] + \Gamma(d[k]) \qquad (2)$$

where $\Phi(d[k])$ and $\Gamma(d[k])$ are matrices that depend nonlinearly on the duty cycle $d[k]$, calculated by integrating the converter equations from $t = k$ to $t = k+1$.

Expression (2) is approximated by determining the matrices $\bar{A}_i$, $\bar{B}_i$ and $\bar{f}_i$ that describe the system in terms of

$$x'[k+1] = \bar{A}_i x'[k] + \bar{B}_i d[k] + \bar{f}_i \qquad (3a)$$
$$\text{if } d[k] \in D_i \quad i = 1, \ldots, \nu \qquad (3b)$$
$$0 \leq d[k] \leq 1 \qquad (3c)$$

and that minimize the sum of quadratic error terms

$$(\Phi(d[k])x'[k] + \Gamma(d[k]) - (\bar{A}_i x'[k] + \bar{B}_i d[k] + \bar{f}_i))^2 \quad (4)$$

over a gridded series of points $x'[k]$ in the state space $[0, i'_{\ell,max}] \times [0, v'_{o,max}]$, where D_i are the ν intervals

$[0, \frac{1}{\nu}], ..., [\frac{\nu-1}{\nu}, 1]$, and $i'_{\ell,max}$, $v'_{o,max}$ are the maximum values of the scaled inductor current and output voltage.

B. KTH: Sampled Data (SD) Modeling

The control synthesis is based on a sampled data (SD) model of the boost converter. The SD model provides a precise description of the system dynamics at the switching instances and it allows the effect of continuous time disturbances and model uncertainty to be exactly accounted for in an equivalent discrete time model.

Within the SD framework we consider $\mathcal{H}_\infty$-synthesis and we therefore include an external disturbance w in the dynamics. The disturbance is chosen as an independent current source at the output to model uncertainty in the load.

To derive the SD model two types of sampling are introduced. Firstly, the ideal sampler S is defined according to $(Sf)[k] := f(kT_s)$ Secondly, the averaging sampler S_{ave} is defined according to

$$(S_{\text{ave}} f)[k] := \frac{1}{T_s} \int_{(k-1)T_s}^{kT_s} f(t) \, dt.$$

The quantities that are sampled are the inductor current i_l and the output voltage v_o. We define

$$\psi_1[k] = (S_{\text{ave}} v_o)[k], \ \psi_2[k] = (SHx)[k] = \begin{bmatrix} i_l(kT_s) \\ v_o(kT_s) \end{bmatrix} \quad (5)$$

The control objective is to ensure asymptotic convergence to a nominal periodic solution (x^0, d^0) that satisfies the tracking condition

$$\lim_{k \to \infty} \frac{1}{T_s} \int_{(k-1)T_s}^{kT_s} v_o(t) \, dt = \int_0^{T_s} v_o^0(t) \, dt = \mathsf{v}_{\text{ref}}. \quad (6)$$

We want (6) to be satisfied robustly against e.g., parameter uncertainties and the disturbance w, and this motivates us to introduce the integrator state

$$e_d[k] := \sum_{i=0}^{k-1} (\psi_1[i] - v_{\text{ref}})$$

and consider the objective of satisfying

$$\int_0^t \left\| \xi(t) - \xi^0(t) \right\|_2^2 \, dt + \sum_{k=0}^{\infty} q \| e_d[k] \|^2 \leq \gamma^2 \int_0^t \| w \|_2^2 \, dt \quad (7)$$

for all $t \geq 0$ and for all solutions to the dynamics in (1). Here, ξ is an auxiliary output that is chosen to tune the controller and ξ^0 corresponds to a stationary periodic solution (x^0, d^0) for the nominal system, i.e. when $w \equiv 0$.

To solve the problem of satisfying (7) subject to the dynamics in (1) we derive a lifting representation of the system, see [4] for details.

C. LTH: Robust Piecewise Affine (RPWA) Systems

Fixed frequency pulse-width-modulated systems are inherently discrete. This is because we can only make control decisions at discrete time instances, $k := T_s k \geq 0$. The

exact state propagation between time k and $k+1$ can easily be obtained by integrating (1) over one period, we obtain

$$x[k+1] = \Phi(d[k])x[k] + \Gamma(d[k]) \tag{8}$$

The matrices $\Phi(d)$ and $\Gamma(d)$ depend nonlinearly on the duty cycle in such a way that the model is not suitable for control synthesis purpose. In addition, these matrices also depend on the output load r_o, which is assumed to be unmeasurable. To resolve these two problems simultaneously we will make a RPWA approximation of the model. To obtain a model that is useful in combination with our synthesis approach we first subdivide the range D of the duty cycle into a finite number of sets D_m such that $\cup D_m = D$. To each D_m we will compute a constant affine system

$$x[k+1] = \Phi_m x[k] + \Gamma_m d[k] + \nu_m \tag{9}$$

valid for $d \in D_m$. When the model (8) is replaced by (9) the largest error we make can be expressed as

$$J = \sup ||\Phi_m x + \Gamma_m d + \nu_m - (\Phi(d, r_o)x + \Gamma(d, r_0))||$$

where the supremum is taken over $(x, d, r_0) \in X \times D_m \times R$, where X is the set of states were the model is valid and R is a model of the set of values the load can assume. Naturally, we would like minimize J. The robust approximation problem is to minimize $J(\Phi_m, \Gamma_m, \nu_m)$ over $(\Phi_m, \Gamma_m, \nu_m)$. Our ability to solve this problem depend on the choice of norm and the description of the set $X \times D_m \times R$, the candidates are those which makes the resulting problem a finite dimensional convex optimization problem, see [5] for examples.

D. Supélec: Port Control Hamiltonian for Affine Systems

The control synthesis using a stabilizing approach is based on a continuous model of the switching system. The Port Control Hamiltonian (PCH) formulation that is used in the control method enables taking into account energetic considerations and it has the following standard expression:

$$\dot{x} = [J(\rho) - R(\rho)]\frac{\partial H(x, \rho)}{\partial x} + G(\rho)u \tag{10}$$

$x = [p_l \ q_c]^T$ is the state vector with p_l the fluxes in the inductances and q_c the charges in the capacitors, ρ is the boolean control variable, J the skew-symmetric intercon-nection matrix, R the symmetric dissipation matrix, H the energy stored in the system, G the power input matrix.

If the constitutive relations of the storage elements are linear, which is most often the case of power converters, the Hamiltonian of the system is:

$$\frac{\partial H(x, \rho)}{\partial x} = Fx = z \tag{11}$$

where $F = F^T > 0$ and in the simple cases, it is a diagonal matrix and $z = [i_\ell \ v_c]^T$ is the co-state vector. Furthermore, in the case of dc-dc power converters, the state equation is affine with respect to boolean control variables [6]. The matrices $J(\rho)$, $R(\rho)$ and $G(\rho)$ can thus be written as:

$$J(\rho) = J_0 + \sum_1^p \rho_i J_i, R(\rho) = r_o + \sum_1^p \rho_i R_i$$

$$G(\rho) = G_0 + \sum_1^p \rho_i G_i \tag{12}$$

where ρ_i are the components of the control vector ρ and p is its dimension.

IV. THE CONTROL PROBLEM

The main control objective for the boost dc-dc converter is to regulate the dc component of the output voltage v_o to its reference $v_{o,ref}$. This regulation has to be achieved in the presence of the hard constraints on the manipulated variable (the duty cycle) which is bounded between 0 and 1, and needs to be maintained despite the changes in the load r_o and the source voltage v_s. Moreover, the controller must render a steady state operation under a constant duty cycle, thus avoiding the occurrence of fast-scale instabilities (subharmonic oscillations).

However, one needs to account for the fact that the output voltage exhibits a non-minimum phase behavior with respect to the duty cycle [7], and for the existence of multiple steady-state equilibria due to the existence of the parasitic elements r_c and r_ℓ [8], the inclusion of which in the model is of crucial importance, as depicted in Fig. 2. Indeed, neglecting them leads to a model that yields an arbitrarily high output voltage for duty cycles close to unity, whereas it can be clearly seen that a realistic setup will yield significantly different results. For an assigned average voltage ratio $\frac{v_o}{v_s} > 1$ there will always be two possible stationary values for the duty cycle for a typical boost converter configuration.

These two problems can be bypassed by formulating the control problem of the boost dc-dc converter as a current (rather than a voltage) regulation problem, aiming at steering the the inductor current to a reference $i_{\ell,ref}$. This approach is the common industrial practice [7], and yields satisfactory results in terms of the closed-loop performance for the following reasons: (i) the inductor current has a minimum phase behavior with respect to the duty cycle [7], and (ii) the steady state characteristic of the average value of i_ℓ is monotonically increasing as a function of the duty cycle. This implies that the region of high duty cycles is to be avoided for the steady state operation of the converter, since due to the high currents the efficiency of the converter drops significantly [8]. Therefore, despite the fact that there will always be two possible stationary values for the duty cycle for a given output voltage reference $v_{o,ref}$, the current corresponding to the lower duty cycle can be selected and taken as the reference $i_{\ell,ref}$.

V. PROPOSED CONTROL APPROACHES

A. ETH: Model Predictive Control

The major advantage of Model Predictive Control (MPC) is its straight-forward design procedure [9]. Given a model of the system, including constraints, one only needs to set up an objective function that incorporates the control objectives.

(a) Ideal case characteristic, with the parasitic elements ignored

(b) Real case characteristic, with the parasitic elements included - the dotted line represents the loci of the points $(d_{max}, \overline{v}_{o,max})$ for a varying r_o
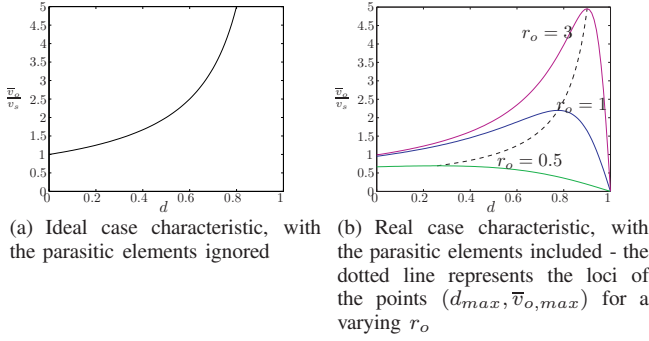
Fig. 2: Input-output steady state characteristic of the step-up converter

The control objectives are to regulate the average output voltage to its reference as fast and with as little overshoot as possible, or equivalently, to minimize the absolute scaled inductor current error $i'_{\ell,err}[k] = |i'_\ell[k] - i'_{\ell,ref}|$. Let $\Delta d[k] = |d[k] - d[k-1]|$ indicate the absolute value of the difference between two consecutive duty cycles. This term is introduced in order to reduce the presence of unwanted chattering in the input when the system has almost reached stationary conditions. Define the penalty matrix $Q = \text{diag}(q_1, q_2)$ with $q_1, q_2 \in \mathbb{R}^+$ and the vector $\varepsilon[k] = [i'_{\ell,err}[k], \Delta d[k]]^T$. Consider the objective function

$$J(D[k], x'[k], d[k-1]) = \sum_{l=0}^{L-1} \|Q\, \varepsilon[k+l|k]\|_1 \qquad (13)$$

penalizing the predicted evolution of $\varepsilon[k+l|k]$ from k over the horizon L using the 1-norm. The control input at time-instant k is then obtained by minimizing the objective function (13) over the sequence of control moves $D[k] = [d[k], \ldots, d[k+L-1]]^T$ subject to the model equations and constraints (3a), (3b), (3c); the resulting optimization program is referred to as the constrained finite time optimal control (CFTOC) problem.

Multi-parametric programming is employed to solve an optimization problem off-line for a range of parameters. In [10] it is shown how to reformulate and solve a discrete-time CFTOC problem for a PWA system as a multi-parametric program featuring the state vector as a parameter. Note that the CFTOC problem is not only a parametric function of $x[k]$, but also of the last control move $d[k-1]$; furthermore, as it is necessary to solve the CFTOC problem for all possible values of $i'_{\ell,ref}$, the scaled inductor current reference also enters the augmented state vector, which therefore results in being 4-dimensional. Again, it should be noticed that normalizing the system equations over v_s allows to define a model independently of the voltage source, and therefore an explicit state-feedback law that depends on one parameter less [11]. As proven in [10] the optimal state-feedback control law $d^*[k]$ is a PWA function of the (augmented) state vector defined on a polyhedral partition of the feasible (augmented) state space. As a result, such a state-feedback controller can be implemented online, since computing the control input amounts to determining the polyhedron in

which the measured state lies and then simply evaluating the corresponding affine control law.

To account for load resistance variations, an estimation scheme is derived. The aim is to use the previously derived state-feedback controller (for a time-invariant and nominal load), augmented by an external loop which adjusts the inductor current reference to compensate for the model mismatch [12].

B. KTH: Sampled-data $\mathcal{H}_\infty$-control

Our goal is to achieve robustness to uncertainty and disturbances in the load and to deal with more complex loads than purely resistive. We therefore prefer voltage regulation to current regulation. The non-minimum phase behavior can be made less pronounced by including both the inductor current and the output voltage in the $\mathcal{H}_\infty$-criterium (7).

The lifted system discussed in the previous section depends on $d[k]$ in a highly nonlinear fashion. We thus linearize the system around d^0 and consider a quadratic approximation of the design criterion (7). The result is a new type of sampled-data $\mathcal{H}_\infty$ control problem which was solved in [4]. For the step-up converter we derived a state feedback controller. The full state is not measured, but can be obtained nominally by inverting ψ_2 in (5), i.e. $x(kT_s) = H^{-1}\psi_2[k]$. To verify that the linear quadratic approximation is a valid we perform a stability analysis of the closed loop system below.

The boost converter is designed to increase the input voltage. It is therefore fair to describe the case when $v_s \geq v_o$ as being out of the normal mode of operation. To increase performance, whenever $v_s^0 \geq v_o$, where v_s^0 is the nominal value of the source voltage, the sampled data controller K is disregarded and we let $d_k = 0$, i.e. we use the control law

$$d_k = \begin{cases} \text{sat}_{[0,d_{\max}]}\left(\mathsf{d}^0 + K(\bar{x}[k] - \bar{x}^0)\right), & v_o \geq v_s^0 \\ 0, & v_o < v_s^0 \end{cases}.$$

where sat is a saturation, $d_{\max}$ is the point where the slope of the $\bar{v}_o/d$-characteristics in Fig. 2(b) changes sign and

$$\bar{x}[k] = \left[(H^{-1}\psi_2[k])' \quad \psi_1[k] \quad e_d[k]\right]', \quad \bar{x}^0 = \begin{bmatrix} x^{0'} & v_{\text{ref}} & 0 \end{bmatrix}'$$

Finally, we add an anti-windup structure. If the linear feedback saturates, then the term

$$\Delta = \mathsf{d}^0 + K(\bar{x}[k] - \bar{x}^0) - d_k$$

is used to modify the integrator state in a linear fashion;

$$e_d[k+1] = e_d[k] + (\psi_1[k] - v_{\text{ref}}) + c\Delta$$

where $c > 0$.

1) Stability analysis: The $\mathcal{H}_\infty$ synthesis was based on a linearization of the system dynamics and the resulting feedback was augmented with nonlinear control structures. To justify the congregate controller a stability analysis was performed using piece wise quadratic Lyapunov functions and a griding procedure as described in [13]. It was shown that the closed loop is globally exponentially stable, see [**?**].

C. LTH: Relaxed Dynamic Programming

1) Relaxed Dynamic Programming: Except for special cases, the computations required to solve a synthesis problem by means of dynamic programming are prohibitive. The only possibility is to resort to approximations. One such formulation was proposed in [14]. Using this formulation, different parametrization of the value function results in different algorithms. In this paper we will use the algorithm proposed by the author in [15]. This algorithm uses a min-max of linear functions as parametrization. In the next section we summarize the properties of this approach in terms of needed computations and the resulting control law.

2) Min-max parametrization: As discussed in the modeling section we assume that the system is given by finite number of affine systems (9). To apply dynamic programming we need to define a suitable step cost $l(x, u)$. Here we consider the l_1-norm. A crucial point for us is that this norm can be represented as a max of linear functions

$$l(x, u) = \left\|W \begin{bmatrix} x \\ u \\ 1 \end{bmatrix}\right\|_1 = \max_{q \in Q} q^T \begin{bmatrix} x \\ u \\ 1 \end{bmatrix} \qquad (14)$$

for some choice of a finite set Q. We use relaxed value iteration to solve for a stationary approximate value function. Suppose that the k'th value function has the following min-max representation

$$V_k(x) = \min_{j \in J_k} \max_{p \in P_{jk}} p^T \begin{bmatrix} x \\ 1 \end{bmatrix} \qquad (15)$$

where J_k and P_{jk} are finite sets. It can be shown, see [15], that the $k + 1$'th value function also is a min-max of linear function. The procedure can be iterated to obtain an approximation which satisfies

$$\beta V^* \leq \hat{V} \leq \alpha V^*$$

where $\beta \leq 1 \leq \alpha$ are constants and V^* is the infinite horizon cost function. Our approach to update the value function in each iteration involves extreme point enumeration of a certain polyhedron, in general such computations are very costly. By exploiting structure, this step is not so costly for us. Instead the most costly step is to solve a linear program.

3) Constraints and feedback control law: It should be noted that the proposed algorithm allows for explicit incorporation of constraints on states and control variables, as long as these can be described by polytopes. Moreover, the function $\hat{V}$ defined by the sets J and P_j, defines an explicit feedback controller $\mu(x)$ which can be implemented in a look-up table. This is so because to every $p \in P_j$ and every $j \in J$ there is a corresponding vector L_p such that $\mu(x) = L_p^T[x^T \quad 1]^T$, hence the controller is piecewise affine. All the L_p's are computed along with $\hat{V}$.

D. Supélec: Stabilizing Control

1) General method: The approaches in the literature which are based on Lyapunov function consider, in general, linear systems with 0 as a common equilibrium point [16], [17]. In the case of power converters, each configuration may or may not have a different equilibrium point and physical considerations enable establishing a common Lyapunov function.

The control objective is expressed using an admissible reference x_0 which must satisfy the constraint:

$$0 = (J(\rho_0) - R(\rho_0)) z_0 + G(\rho_0) E \qquad (16)$$

with $\rho_0 \in \mathbb{R}^p, 0 \leq \rho_{0i} \leq 1$, $z_0 = Fx_0$. According to the properties of this equation and the respective dimension or x and ρ, for one ρ_0, the equilibrium point can be unique or not, and for ρ_0 any point of the state space can be an equilibrium point or not [18].

For a function V to be a Lyapunov function for a system in a point x_0 it must be positive anywhere except in x_0 and its derivative must not be strictly positive. The candidate Lyapunov function has the following form:

$$V(x, x_0) = \tfrac{1}{2} (x - x_0)^T F (x - x_0) \qquad (17)$$

Since the matrix F is positive, V is positive and continuous for every x and it is null only in x_0. Its derivative depends on the control variable and using (10) and (16) it can be expressed as following:

$$\dot{V}_\rho = -(z - z_0)^T R(\rho)(z - z_0) + \sum_1^p T_i(\rho_i - \rho_{0i}) \quad (18)$$

with:

$$T_i = (z - z_0)^T ((J_i - R_i) z_0 + g_i u), i = 1 : p \qquad (19)$$

Due to the fact that $R(\rho)$ is a non-negative matrix, the first term is always negative, and because $0 \leq \rho_{0i} \leq 1$ the sum can be made negative by choosing an appropriate value for each ρ_i according to the sign of each T_i.

Various methods can be conceived to assure the negativity of (18). In the following, a maximum descent strategy will be used, which consist in choosing a new value for the control variable each time one T_i changes its sign. This defines commutation surfaces in the state space, $T_i = 0$, along which the system has a sliding motion [18].

2) Control of frequency: Because this strategy requires an infinite bandwidth a dead-zone is created with the help of a parameter ϵ. This way the derivative of the Lyapunov function may take positive values for a limited amount of time. The new commutation surfaces are thus defined by $T_i = \epsilon$. The period and the amplitude of the oscillations around the reference are determined by this parameter. To maintain a constant frequency, in the case of parameter variations, a discrete PI controller is used to compute the value for ϵ, having as input the period of the control signal.

3) Application to the Step-up DC-DC converter: The admissible reference is calculated as in (16) for a value of 1 p.u. for the voltage. The low value for the current is chosen when selecting z_0. As there is only one control variable, the sum from expression (18) has only one term T, which, according to (19) becomes:

$$T = \frac{r_o i_0}{r_c + r_o}(v - v_0) - \frac{r_o r_c i_0 + r_o v_0}{r_c + r_o}(i - i_0) \qquad (20)$$

VI. SIMULATION RESULTS

In this section we present a simulation study where each suggested control strategy is tested. All simulations are done using the same Simulink code and use the same set of plant parameters. The output voltage reference is always $v_{o,ref} = 1$ while the circuit parameters, expressed in the per unit system, are given by $x_c = \frac{70}{2\pi}$ p.u., $x_\ell = \frac{3}{2\pi}$ p.u., $r_c = 0.005$ p.u. and $r_\ell = 0.05$ p.u.. If not otherwise stated, the source voltage is set to $v_s = 0.75$ p.u. and the output resistance is given by $r_o = 1$ p.u.. We should note here that current limit protection in the case of a short circuit in the load is not possible for the step-up converter. Therefore, we have not included such a case study in the proposal.

The case studies that have been considered are the following:

1) The first case concerns the start-up of the converter from zero initial conditions, i.e. with initial state $x(0) = [0, \ 0]^T$ to the desired steady state operation point.

2) In the second case, the response of the converter to source voltage variations is tested. The converter is initially at steady state with $v_s = 0.5$ p.u. when a step change to $v_s = 0.9$ p.u. is applied.

3) The third case examines the response of the converter to step changes in the output load. Starting from the steady state, the load steps up at a given time-instant from $r_o = 1$ p.u. to $r_o = 1.5$ p.u..

A. ETH: Model Predictive Control

The model was derived for a range of values of $[0, 4]$ for the scaled inductor current and $[0, 3]$ for the scaled output voltage; three PWA dynamics were calculated, with the intervals D_i being $[0, \frac{1}{3}]$, $[\frac{1}{3}, \frac{2}{3}]$, and $[\frac{2}{3}, 1]$. For the cost function, the penalty matrix is chosen to be $Q = \mathrm{diag}(10, 1)$ and the prediction horizon in all cases is $L = 2$. As explained in Section V-A the explicit state-feedback controller is defined in a 4-dimensional space resulting in a polyhedral partition consisting of 239 regions, which, by utilizing the merging algorithm introduced in [11] can be simplified to 121 regions.

Fig. 3 depicts the response of the proposed optimal control scheme during start-up, yielding an output voltage that reaches its stationary conditions with an overshoot of about 4% and within 10 switching periods. For the
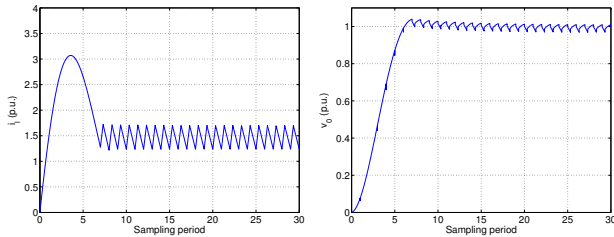

Fig. 3: ETH: Closed loop step response from zero initial conditions

second case the results are shown in Fig. 4; the new value
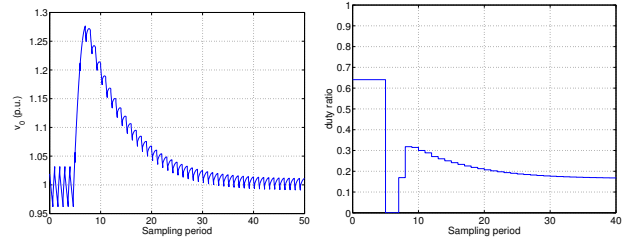

Fig. 4: ETH: Closed loop response to a step in the source voltage from $v_s = 0.5$ p.u. to $v_s = 0.9$ p.u.
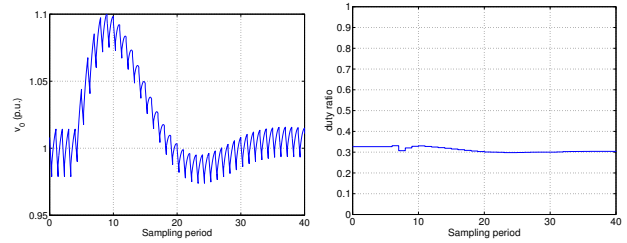

Fig. 5: ETH: Closed loop response to a step in the load resistance from $r_o = 1$ p.u. to $r_o = 1.5$ p.u.

of the voltage source is measured, the current reference updated accordingly and the system restored to its desired output voltage value. Simulations from the final case are displayed in Fig. 5. The Kalman filter adjusts the current reference and the output voltage reaches its desired value after approximately 20 switching periods.

B. KTH: Sampled-Data Control

In the controller design the signal ξ was chosen as

$$\xi = \begin{bmatrix} 1.6 & 8 \end{bmatrix} x$$

and the remaining design parameters are $q = 11.5$ and $\gamma = 0.5$. The parameter of the anti windup feedback is $c = 0.5$. We notice that we only use the output voltage and the inductor current for control. It would also be possible to use a dynamic feedback law and then only use the output voltage for control and still get satisfactory performance.

The simulation in Fig. 6 shows the transient behavior during startup, see Fig. 6. The output voltage reaches the reference level with an overshoot of 5%. The simulations in Fig. 7 and in Fig. 8 show the response to a source voltage and a load resistance increase, respectively.
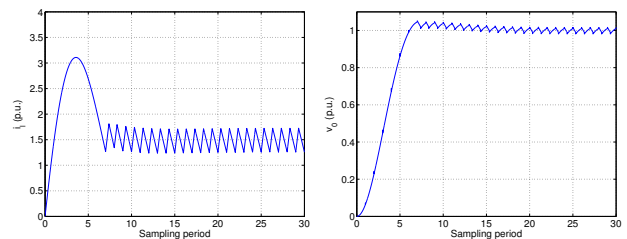

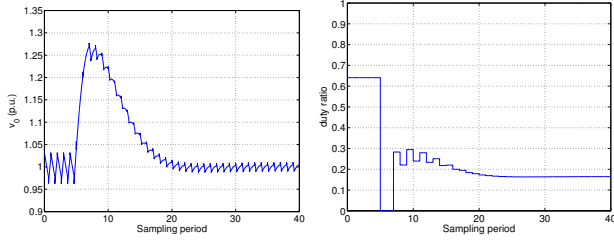Fig. 6: KTH: Closed loop step response from zero initial conditions

Fig. 7: KTH: Closed loop response to a step in the source voltage from $v_s = 0.5$ p.u. to $v_s = 0.9$ p.u.
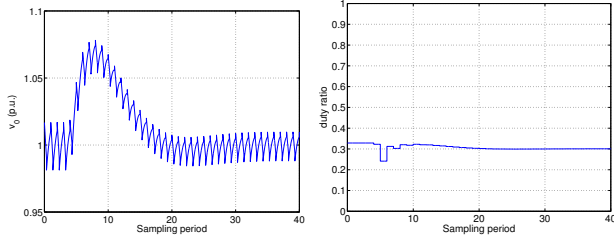

Fig. 8: KTH: Closed loop response to a step in the load resistance from $r_o = 1$ p.u. to $r_o = 1.5$ p.u.

C. LTH: Relaxed Dynamic Programming

We used the approach in section III-C to compute an approximate model consisting of two affine systems. As explained in section V-C it is a good idea to control the current to a suitable reference value i_{ref}. A simple, and yet effective, way to compensate for errors in the model is to introduce an integrator state. Since we would like regulate the current to i_{ref} we augment (8) with an error state

$$e[k+1] = e[k] - i[k] + i_{ref} \qquad (21)$$

This integrator state can now be used for feedback, and thus the controller will have integral action. We used the step cost

$$l(x, e, \hat{d}, d) = q_1|i_{ref} - i| + q_2|e| + q_3|d - \hat{d}| \qquad (22)$$

where $\hat{d}$ is last control value and q_1, q_2 and q_3 are non-negative parameters chosen to reflect the relative importance of the different terms in l. The reason to introduce the extra state $\hat{d}$ is to avoid subharmonic oscillations at stationary conditions.

Our simulations are shown in figures 9-11. As can be seen the step response is fast, it reaches its reference value after only 6 cycles and makes an overshoot of 5%. The mean value is within 1% already after 11 cycles. The fast repsonse is due to our choice of relatively high value on q_1, as compared to q_2 and q_3.

The response to an increase in the voltage source v_s from 0.5 p.u. to 0.9 p.u. during steady state operation are shown in Fig. 9. As the new value of v_s becomes available to the controller a new current reference value is computed. The ringing in the control signal the first 15 cycles is, again, due to the high relative penalty on the current error.

In the final case we a 50% increase in the load resistance r_o from 1 p.u. to 1.5 p.u. is imposed during steady state operation. The results are shown figure 11. An assumed

estimator adjusts the current reference and the output voltage reaches its desired value after approximately 20 switching periods.
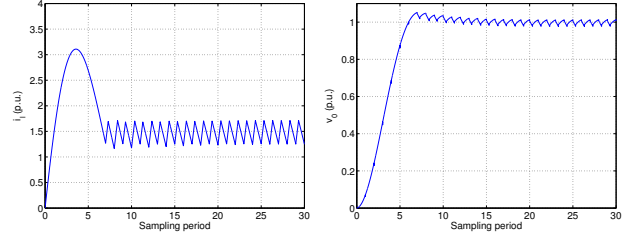

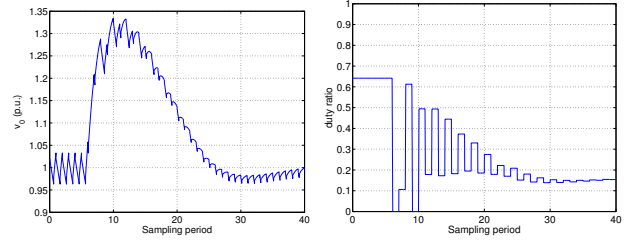Fig. 9: LTH: Closed loop step response from zero initial conditions

Fig. 10: LTH: Closed loop response to a step in the source voltage from $v_s = 0.5$ p.u. to $v_s = 0.9$ p.u.
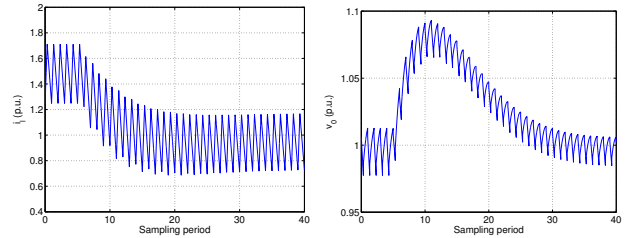

Fig. 11: LTH: Closed loop response to a step in the load resistance from $r_o = 1$ p.u. to $r_o = 1.5$ p.u.

D. Supélec: Stabilizing Control

In this section, simulation results demonstrating the performance of the stabilizing control methodology are presented. As explained in section V-D the goal is to assure the negativity of the Lyapunov function candidate (17) by choosing a value for the control variable at each instant when the term (20) becomes greater than a parameter ϵ. Since the command signal for the switch is directly imposed, this results in a scheme with a variable switching frequency; for the sake of comparison a *pseudo* duty cycle, defined as the average over one switching period of the amount of time the switch is kept on, is calculated and presented in the following plots alongside the command signal. Results for the startup are depicted in Figure 12; Figure 13 depicts the response of the controlled system in the case of an increase in the source voltage from 0.5 p.u. to 0.9 p.u.. The new value for the admissible reference is recalculated and the output of the system is restored to the desired output with an overshoot of
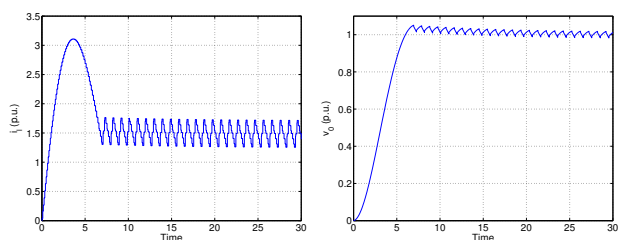
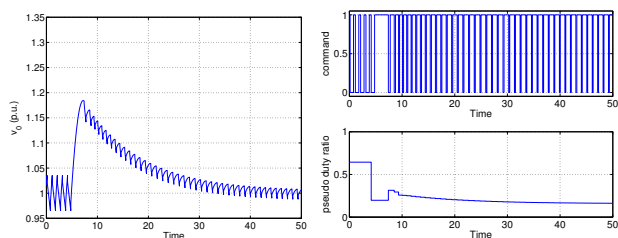Fig. 12: Supélec: Closed loop step response from zero initial conditions

Fig. 13: Supélec: Closed loop response to a step in the source voltage from $v_s = 0.5$ p.u. to $v_s = 0.9$ p.u.
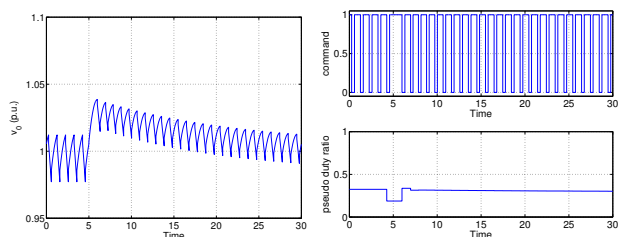

Fig. 14: Supélec: Closed loop response to a step in the load resistance from $r_o = 1$ p.u. to $r_o = 1.5$ p.u.

under 20%. Figure 14 depicts the response of the controlled system in the case of an increase of the load from 1 p.u. to 1.5 p.u.. The variation is supposed to be measurable, and in each case a new value for the admissible reference is recalculated and the output of the system is restored to the desired value.

VII. COMPARISONS AND CONCLUSIONS

In this paper a collective study of different hybrid control techniques applied to the same benchmark example of a step-up dc-dc converter has been presented. The solution approaches proposed in the paper are all based on digital control techniques where measurement and actuation take place only at the sampling instances.

The methods presented by ETH, LTH and KTH all act at the beginning of each switching period and use the duty cycle as the manipulated variable, rendering a constant switching frequency operation; the former two allow for a more systematic analysis of the circuit characteristics but typically yield an increased degree of complexity in the controller, whereas the latter might be suitable for higher switching frequencies in view of its more affordable implementation requirements. The method of Supélec, on the other hand, directly decides on the discrete position of the controlled switch based on a

much faster sampling of the system, and results in a scheme with an improved behavior during transient, but also with a variable switching frequency. In this case, the operation under an excessively high switching frequency is avoided through the use of an outer PI loop that adjusts the deadband between the commutation surfaces. It is the opinion of the authors that the trade-off between this performance improvement and the disadvantages of the variable switching frequency operation (especially with respect to the converter's EMI design), can only be judged on an applicationspecific basis. Future research directions will be focused on extending the presented methods to more complicated converter topologies and on strategies for dealing with the parameter variations and dynamic uncertainties appearing under experimental conditions.

VIII. ACKNOWLEDGEMENTS

REFERENCES

[1] M. Morari, J. Buisson, B. de Schutter, and G. Papafotiou, "Final report on modeling tools, benchmarks and control methods," HYCON Deliverable, Tech. Rep. IST contract number 511368, 2006, http://control.ee.ethz.ch/hycon/downloads_free/HYCON_D4a31.pdf.
[2] R. Middlebrook and S. Ćuk, "A general unified approach to modeling switching power converter stages," *IEEE Power Electronics Specialists Conference Records*, pp. 18–34, 1976.
[3] R. Erickson, S. Ćuk, and R. Middlebrook, "Large signal modeling and analysis of switching regulators," *IEEE Power Electronics Specialists Conference Records*, pp. 240–250, 1982.
[4] H. Fujioka, S. Almér, U. Jönsson, and C.-Y. Kao, "Control synthesis for a class of PWM systems for robust tracking and $\mathcal{H}_\infty$ performance," in *Proceedings of the IEEE Conf. Decision & Control*, 2006, to appear.
[5] S. Boyd and L. Vandenberghe, *Convex Optimization*. Cambridge University Press, 2004.
[6] J. Buisson, H. Cormerais, and P. Y. Richard, "Analysis of the bond garph model of hybrid physical systems with ideal swithces," *Journal of Systems and Control Engineering*, no. 11, November 2002.
[7] N. Mohan, T. M. Undeland, , and W. P. Robbins, *Power Electronics: Converters, Applications and Design*. Wiley, 1989.
[8] G. T. Kostakis, S. Manias, and N. Margaris, "A generalized method for calculating the rms values of switching power converters," *IEEE Transactions on Power Electronics*, vol. 15, pp. 616–625, 2000.
[9] J. Maciejowski, *Predictive Control*. Prentice Hall, 2002.
[10] F. Borrelli, *Constrained Optimal Control of Linear and Hybrid Systems, Volume 290 of Lecture Notes in Control and Information Sciences*. Springer, 2003.
[11] T. Geyer, "Low complexity model predictive control in power electronics and power systems," Ph.D. dissertation, ETH Zurich, 2005.
[12] A. G. Beccuti, G. Papafotiou, and M. Morari", "Explicit model predictive control of the boost converter," ETH Zurich, Tech. Rep., 2006. [Online]. Available: www.control.ee.ethz.ch
[13] S. Almér, U. Jönsson, C.-Y. Kao, and J. Mari, "Global stability analysis of DC-DC converters using sampled-data modeling," in *American Control Conference*, 2004.
[14] B. Lincoln and A. Rantzer, "Suboptimal dynamic programming with error bounds," in *Proc. 41st IEEE Conference on Decision and Control*, Dec. 2002.
[15] A. Wernrud, "Min-max parametrization of value functions." Department of Automatic Control, Lund University, Tech. Rep., in preparation.
[16] R. DeCarlo, M. Branicky, S. Petterson., and B. Lennartson, "Perspectives and results on the stability and stabilisability of hybrid systems," *Proceedings of the IEEE*, no. 88, pp. 1069–1082, 2003.
[17] D. Liberzon and A. S. Morse, "Basic problems in stability and design of switched systems," *IEEE Control Systems Magazine*, no. 19, 1999.
[18] J. Buisson, H. Cormerais, and P. Y. Richard, "On the stabilization of switching electrical power converters," *Hybrid Systems: Computation and Control*, March 2005.